Geochimica et Cosmochimica Acta Vol. 55, pp. 471–482

0016-7037/91/$3.00 + .00

Pyrite oxidation at circumneutral pH

CARL O. MOSES* and JANET S. HERMAN
Department of Environmental Sciences, University of Virginia, Charlottesville, VA 22903, USA

(*Received October* 24, 1989; *accepted in revised form November* 20, 1990)

Abstract—Previous studies of pyrite oxidation kinetics have concentrated primarily on the reaction at low pH, where Fe(III) has been assumed to be the dominant oxidant. Studies at circumneutral pH, necessitated by effective pH buffering in some pyrite oxidation systems, have often implicitly assumed that the dominant oxidant must be dissolved oxygen (DO), owing to the diminished solubility of Fe(III). In fact, $Fe(III)_{(aq)}$ is an effective pyrite oxidant at circumneutral pH, but the reaction cannot be sustained in the absence of DO. The purpose of this experimental study was to ascertain the relative roles of Fe(III) and DO in pyrite oxidation at circumneutral pH.

The rate of pyrite oxidation was first-order with respect to the ratio of surface area to solution volume. Direct determinations of both $Fe(II)_{(aq)}$ and $Fe(III)_{(aq)}$ demonstrated a dramatic loss of Fe(II) from the solution phase in excess of the loss for which oxidation alone could account. Based on rate data, we have concluded that Fe(II) is adsorbed onto the pyrite surface. Furthermore, Fe(II) is preferred as an adsorbate to Fe(III), which we attribute to both electrostatic and acid-base selectivity. We also found that the rate of pyrite oxidation by either $Fe(III)_{(aq)}$ or DO is reduced in the presence of aqueous Fe(II), which leads us to conclude that, under most natural conditions, neither $Fe(III)_{(aq)}$ nor DO directly attacks the pyrite surface.

The present evidence suggests a mechanism for pyrite oxidation that involves adsorbed Fe(II) giving up electrons to DO and the resulting Fe(III) rapidly accepting electrons from the pyrite. The adsorbed Fe is, thus, cyclically oxidized and reduced, while it acts as a conduit for electrons traveling from pyrite to DO. Oxygen is transferred from the hydration sphere of the adsorbed Fe to pyrite S. The cycle of adsorbed Fe oxidation and reduction and the successive addition of oxygen to pyrite S continues until a stable sulfoxy species dissociates from the surface. Prior work has shown that sulfoxy species of lower oxidation state than sulfate (e.g., thiosulfate or polythionate) may accumulate in solution under some circumstances but not under the conditions of the experiments reported here. In these experiments, the rate of sulfate accumulation in solution is proportional to the rate of pyrite oxidation.

INTRODUCTION

IRON AND SULFUR rank fourth and fifteenth, respectively, among the elements in their crustal abundance (MASON, 1966). In addition to their abundance, their redox reactivity accounts for the variety of geochemical processes in which they are involved and for their importance in biological systems. Throughout Earth's history, the biogeochemical cycles of iron and sulfur have been inextricably interwined through the deposition and weathering of iron sulfide minerals. Of these minerals, the most common is pyrite.

Aside from its role in ancient and modern biogeochemical cycles of iron, sulfur, oxygen, and carbon (HOLLAND, 1978; BERNER et al., 1983; HOLLAND, 1984; BERNER and BERNER, 1987), pyrite weathering has modern-day significance as a potential degrader of water quality, often yielding high acidity and concentrations of metals and sulfate that exceed water-quality standards. Such pyrite weathering, typified by acid mine drainage, is often a consequence of human activities, such as mining or the processing of coal or metal ores (e.g., CLARK, 1966; CARUCCIO, 1975; KLEINMANN and CRERAR, 1979). Natural sulfide mineral weathering processes that occur, for example, during supergene ore enrichment are also known to generate high levels of their products (GRANGER and WARREN, 1969; THORNBER, 1975; REYNOLDS and GOLDHABER, 1978; CHANTRET and BOULEGUE, 1980). On the other hand, pyrite weathering does not always produce very high levels of acidity or metals because of pH buffering by natural chemical or biological processes, such as carbonate mineral dissolution (TORAN, 1987; NICHOLSON et al., 1988) or bacterial sulfate reduction (HERLIHY et al., 1988). Furthermore, the processes that yield low pH must be initiated in waters of circumneutral (or near-neutral) pH. In this study, we address pyrite oxidation at circumneutral pH where proton and metal concentrations are low.

Pyrite oxidation typically is far from equilibrium, whether represented by reaction (1) (GARRELS and THOMPSON, 1960) or reaction (2) (SMITH et al., 1968), which is the sum of reaction (1) and 14 × reaction (3) (SINGER and STUMM, 1970a).

$$FeS_2 + 14Fe^{3+} + 8H_2O \rightarrow 15Fe^{2+} + 2SO_4^{2-} + 16H^+ \quad (1)$$

$$FeS_2 + {}^7/_2O_{2(aq)} + H_2O \rightarrow Fe^{2+} + 2SO_4^{2-} + 2H^+ \quad (2)$$

$$Fe^{2+} + {}^1/_4O_{2(aq)} + H^+ \rightarrow Fe^{3+} + {}^1/_2H_2O \quad (3)$$

The net forward rate of a reaction can be expected to diminish as it approaches equilibrium more closely, but for a reaction far from equilibrium, there is essentially no reverse rate (and, therefore, no backward arrow in reactions 1–3). The forward rate of pyrite oxidation, thus, determines the amount of

* *Present address:* Department of Geological Sciences, Lehigh University, Bethlehem, Pennsylvania 18015, USA

products produced or pyrite destroyed in a given span of time.

The oxidation of sulfide minerals, particularly pyrite, has been extensively reviewed by HISKEY and SCHLITT (1982), LOWSON (1982), and NORDSTROM (1982). Advances in our understanding of the rates of pyrite oxidation contributed since these reviews include GOLDHABER (1983), MCKIBBEN (1984), WIERSMA and RIMSTIDT (1984), MCKIBBEN and BARNES (1986), MOSES et al. (1987), TORAN (1987), and NICHOLSON et al. (1988).

Of particular pertinence to the present study are the investigations of pyrite oxidation at circumneutral pH in unbuffered solutions by GOLDHABER (1983) and MOSES et al. (1987). The essential feature of the reaction mechanism proposed by GOLDHABER (1983) is the initiation of pyrite oxidation by the direct attachment of a DO molecule to the partially protonated pyrite surface (Fig. 1a, b). It has commonly been assumed that, at circumneutral pH, DO must

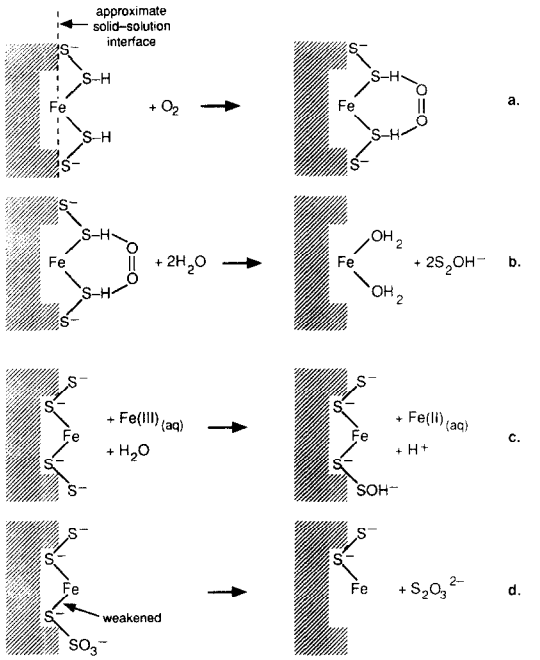

FIG. 1. Schematic comparison of circumneutral-pH pyrite oxidation reactions. (a and b) Oxidation by molecular oxygen (GOLDHABER, 1983). (c and d) Oxidation by $Fe(III)_{(aq)}$ (MOSES et al., 1987). Note that the solid-solution interface is illustrative only; no attempt is made to depict a double layer or a diffuse layer. The molecular oxygen sequence is initiated (a) by the attachment of O_2 to the partially protonated surface, requiring a $pH_{zpc,pyrite} \sim 7$. The second step (b, considered the rate limiting one of the two) requires breaking the double bond in the O_2 and displacement by H_2O of an S_2OH^- molecule. The S_2OH^- is oxidized to sulfate via sulfoxy intermediates including thiosulfate. The $Fe(III)_{(aq)}$ sequence is initiated (c) by the transfer of a hydroxyl group (OH) to a pyrite sulfur atom from the hydration sphere of the aquo-Fe(III) complex in exchange for an electron from the pyrite sulfur atom. The pyrite surface charge, consistent with a low $pH_{zpc,pyrite}$, remains unchanged, and the reduced charge on the Fe is balanced by the proton also released from the hydration sphere. As more hydroxyls are similarly added to the pyrite sulfur and electrons transferred to Fe(III), the Fe-S bond weakens as indicated in (d) until a sulfoxy species is formed that is stable enough in solution to dissociate from the surface (thiosulfate is illustrated).

Table 1. Semi-quantitative spectrographic analysis of pyrite sample.[a]

Si	Mg	Ca	Al	Pb	Mn
~0.4	1500	500	400	400	350
	Zn	Ti	Cu	Ag	
	300	200	50	40	

<100: Be, Bi, Co, Cr, Nb, Ni, Sn, V, Zr

[a]concentrations in ppm, except Si in %

be the direct oxidant (reaction 2) due to the low solubility of Fe(III). SMITH et al. (1968) and MOSES et al. (1987) questioned this assumption, and the latter paper showed that Fe(III) is a very effective pyrite oxidant at circumneutral pH. MOSES et al. (1987) proposed an extension of the Singer-Stumm model of pyrite oxidation (SINGER and STUMM, 1968; 1970a,b) to circumneutral pH (Fig. 1c, d), where the solubility of Fe(III) is so low that the reservoir of $Fe(III)_{(aq)}$ is rapidly depleted by reduction on pyrite, and Fe(II) oxidation becomes rate limiting because it is needed to maintain $Fe(III)_{(aq)}$ concentrations.

The present investigation was designed to further refine the extended Singer-Stumm model of pyrite oxidation by clarifying the roles of DO and Fe(III) in pyrite weathering. The ultimate goals were to determine which oxidant is more directly involved at circumneutral pH and to propose a mechanism for the reaction.

METHODS

Sample Preparation and Characterization

Pyrite was ground from coarse-grained, massive specimens from Rico, Colorado, and separated from nonsulfide phases (mostly quartz). This material is the same pyrite used for the experiments reported by MOSES et al. (1987). All of the results reported here were obtained from experiments using grain sizes in the 38–45 μm fraction. Table 1 presents a semiquantitative spectroscopic analysis of the starting material.

For each experiment, approximately 2.5 g of material was boiled in concentrated HCl, rinsed with boiling concentrated HCl at least twice, and rinsed with boiling acetone at least three times. After the last rinse with boiling acetone, the pyrite was allowed to dry, weighed to the nearest 0.1 mg, and used for the experiment immediately (Method 3 of MOSES et al., 1987).

The specific surface area ($\bar{A}$, $m^2\ g^{-1}$) was determined by three-point fits to a BET isotherm (BRUNAUER et al., 1938) using $N_{2(g)}$ in a Quantasorb BET surface area analyzer (Quantachrome). We determined $\bar{A}$ for a sample of cleaned but unreacted material and for a sample of material that had been used in a 1-h DO-saturated experiment with no added Fe (as described below) and then rinsed with acetone to displace the aqueous reaction solution and to facilitate rapid drying. The manufacturer of the surface area analyzer reports that the measurement error usually does not exceed $\pm 10\%$ ($2\text{–}3\sigma$), but experience with surface areas similar to those obtained for these samples has shown that larger errors are possible (J. D. Rimstidt, pers. comm., 1987).

The grain size distribution of the same two samples was determined with an Elzone particle size analyzer (Particle Data, Inc.). In determining each grain size distribution, $\sim 10^5$ particles were measured, so the precision of the distribution is typically within a few percent (A. Meglis, pers. comm., 1987).

Experimental Procedures

The experiments were carried out in polyethylene titration vessels (Radiometer 956-178) that were mounted on a pH-stat (Radiometer TTA-80 Titration Assembly; for a diagram, see Fig. 1 of MOSES and

HERMAN, 1989). On the pH-stat, separate glass and reference electrodes were used (Radiometer G2040C and K4040), and the pH meter was a Radiometer PHM84. The pH measuring system was calibrated before and after each experiment. Post-experiment calibrations differed from pre-experiment calibrations by <0.02 pH unit. Two titrators were used with two automated 2.5-mL burets (Radiometer TTT60 and TTT80 Titrators and ABU13 and ABU80 Autoburets), so that the pH-stat could respond to both increases and decreases in pH. The titrants were 0.1 *M* LiOH and 0.1 *M* HCl.

The temperature was not controlled, but it was monitored frequently and was found to always fall between 23.0 and 23.5°C.

Iron(II) solutions were prepared by dissolving Fe wire (99.999%, Baker) in low-Fe redistilled HCl (G. F. Smith). The solutions were kept essentially free of Fe(III) by reduction with $H_{2(g)}$ in the presence of palladium black (MOSES et al., 1988).

Reaction solutions were all deaerated 0.01 *M* NaCl, and the reaction solution volume was 40–50 mL. Other experimental conditions are summarized in Table 2. The solution was dispensed to a titration vessel, which was placed on the titration assembly, and the solution was purged with $N_{2(g)}$ while the pH-stat adjusted the pH to the target value. The $N_{2(g)}$ was passed over heated copper wool to remove $O_{2(g)}$. When the target pH was attained, the $t(0)$ sample was withdrawn, the pyrite (~1–2 g) was charged to the vessel, the oxidant was introduced, and the time course was begun.

When the solution was to be sampled, both titrators were halted about 10 sec prior to sampling, the vessel was removed from the titration assembly, the sample was withdrawn, the vessel was replaced on the titration assembly, and the titrators were restarted. The sampling process required <20 sec, during which the pH drifted <0.1 pH unit. pH stasis was restored within a few seconds of restarting the titrators. An Eppendorf micropipet was used to withdraw the samples. The pipet tip was covered with two layers of a polyester screen (33 μm mesh openings, Tetko) to exclude pyrite particles from the sample but admit Fe(III)-oxyhydroxide solids and, thereby, sample total Fe in the system other than pyrite. Two-mL samples were withdrawn and split into aliquots (1 mL each) for Fe and SO_4^{2-} analysis. Samples for Fe analysis were acidified (20 μL 6 *M* HCl) immediately and were analyzed immediately or as soon as the analysis of the previous sample was complete (always within 2 h). When analyses were not immediate, the samples were stored in the dark. Aliquots for SO_4^{2-} analysis received no treatment and were stored at 2–5°C until analysis, which was completed within 48 h of the experiment. Total ΔV for samples removed ranged from 16–22 mL (as high as 50%).

For DO-saturated experiments, the flow rate of the O_2 purge gas was 0.5–1.0 SCFH (specific $ft^3\ h^{-1}$ or ~4–8 mL s^{-1}; the flowmeter was calibrated for Ar), and the total pressure was atmospheric (~1 bar). Experiments were performed with and without added Fe(II). The saturation with respect to DO was determined with duplicate Winkler titrations (APHA, 1976).

Iron(III) solutions for anoxic experiments were prepared from an Fe atomic absorption standard stock solution (1000 mg L^{-1}, Fisher or Scientific Products). These solutions are prepared from $FeCl_3$ and contain essentially no Fe(II) (confirmed by our analysis). The stock solution was diluted with deaerated 0.01 *M* NaCl. During the first half of the time course of the experiment, the solution was purged with N_2, and the purge gas was then switched to O_2 so that the latter half of the experiment was DO-saturated.

Table 2. Conditions for circumneutral-pH pyrite oxidation experiments.

expts	pH	D.O.[a]	Fe(III)[b]	Fe(II)[b]	experiment duration (s)	N[c]
A	6	sat	no	yes	6720–7200	2
B1	6	none	yes	no	1800–1950	4
B2	6	sat	yes	no	3480–4770	4
C	7	sat	no	yes	6360–7440	4
D1	7	none	yes	no	1920	2
D2	7	sat	yes	no	3480	2
E	7	sat	no	no	970–4080	10

[a]sat=saturated, none=anoxic
[b]no=not added, yes=added to reaction solution
[c]number of experiments in group

Iron was analyzed by ion chromatography (IC) by the method of MOSES et al. (1988); each analysis was sensitive to <2 μ*M* Fe. Sulfate was also analyzed by IC. The method of MOSES et al. (1984) was adapted to the use of AG-3 and AS-3 analytical guard and separator columns (Dionex) and an automated sample injector (Varex VRS-201); each analysis was sensitive to <1 μ*M* SO_4^{2-}.

Treatment of Rate Data

Throughout this report, brackets ([· · ·]) are used to denote μ*M* concentrations. Micromolar concentrations of OH^- were obtained from speciation models of the reaction solution computed by WATEQF (PLUMMER et al., 1976). WATEQF calculated the ionic strength of the solution and the activity coefficient of OH^- (using the Davies equation), with which it calculated the molar concentration of OH^- from the pH after accounting for complexation of OH^-. Time is reported in seconds (s), and points during an experimental time course are designated $t(x)$, where x represents a value in seconds.

In all of the experiments, $[SO_4^{2-}]$ was used as the primary reaction progress variable (RPV) for the quantification of reaction rates. In the anoxic experiments, we used $[Fe(III)_{(aq)}]$ as a supplemental RPV that provided a corroborating constraint on the $[SO_4^{2-}]$-based rates. We address the issues of reaction stoichiometry and RPVs in the Discussion.

In formulating a macroscopic rate law, we assumed that the reaction is zero-order in $[SO_4^{2-}]$ and $[Fe(II)_{(aq)}]$, which are reaction products. We did not assume that the reaction is zero-order in $[Fe(III)_{(aq)}]$, [DO], or $[H^+]$, but we did not attempt to measure the order with respect to these species in the present work, so we formulated the rate law with these concentrations held constant, giving zero-order in each of the three for our experiments. We begin our rate law formulation with the assumption that dependence on the ratio of total surface area to reaction solution volume (A/V) is first-order (LASAGA, 1981; this assumption is examined further in the Discussion). With these considerations, we begin by writing the rate expression (Eqn. 4, in which [pyrite] is measured in units consistent with the measurement of $[SO_4^{2-}]$).

$$\text{rate} = \frac{-d\,[\text{pyrite}]}{dt} = \frac{(0.5)d\,[SO_4^{2-}]}{dt}. \tag{4}$$

The (0.5) factor in Eqn. (4) reflects the stoichiometric relationship between moles of pyrite oxidized and moles of SO_4^{2-} produced (reactions 1 and 2). The rate law is the product of the rate coefficient k and the concentration of each species that participates in the reaction raised to a power that reflects the reaction order (Eqn. 5):

$$\text{rate} = k\left(\frac{A}{V}\right)^1 [Fe(II)_{(aq)}]^0[SO_4^{2-}]^0[H^+]^0[Fe(III)_{(aq)}]^0[DO]^0,$$

or

$$\text{rate} = k\left(\frac{A}{V}\right). \tag{5}$$

The rate coefficient was determined from the experimental data by taking the slope of a plot of $(0.5)\left(\frac{V}{A}\right)[SO_4^{2-}]$ vs. t. We refer to the quantity $(0.5)\left(\frac{V}{A}\right)[SO_4^{2-}]$ as the normalized sulfate concentration with units of μmole m^{-2}. The slope was obtained by a linear model (Eqn. 6, derived by combining Eqns. 4 and 5 and integrating), which was fitted to the data by the method of least squares:

$$t = k^{-1}(0.5)\left(\frac{V}{A}\right)[SO_4^{2-}]. \tag{6}$$

Because of our conclusion that the surface area change was negligible (see Discussion), we used the average of the specific surface area

values obtained before and after an experiment (0.066 $m^2 g^{-1}$) when normalizing rates to constant A/V.

When $[Fe(III)_{(aq)}]$ was used as an RPV for the anoxic experiments, the same rate law (Eqn. 5) was assumed to apply. The rate expression was modified to account for the different stoichiometric correction ($^1/_{14} = 0.07$, Eqn. 7, cf. reaction 1):

$$\text{rate} = \frac{-d[\text{pyrite}]}{dt} = \frac{-(0.07)d[Fe(III)_{(aq)}]}{dt}. \quad (7)$$

As with the rate data determined with $[SO_4^{2-}]$ as the RPV (Eqn. 6), the rate coefficient when $[Fe(III)_{(aq)}]$ was the RPV was determined by the slope of a linear model fit to the $(0.07)\left(\frac{V}{A}\right)[Fe(III)_{(aq)}]$ ('normalized' ferric iron concentration) vs. t data (Eqn. 8).

$$t = -k^{-1}(0.07)\left(\frac{V}{A}\right)[Fe(III)_{(aq)}]. \quad (8)$$

A variation on the method of initial rates (LASAGA, 1981) was used to determine the dependence of the reaction on the A/V ratio and test the first-order dependence assumed in the derivation of the rate law (Eqn. 5). Our model was the log transform of the rate law (Eqn. 9), with the reaction order n and the log of the rate coefficient k as parameters to be fit to the data (log rate vs. A/V) by the least squares method:

$$\text{rate} = k\left(\frac{A}{V}\right)^n$$

or

$$\log \text{rate} = \log k + n \log\left(\frac{A}{V}\right). \quad (9)$$

We treated the time interval between each pair of samples as a separate experiment in fitting Eqn. (9) to the data, and we computed the rate for each interval as the finite-difference approximation $\Delta[SO_4^{2-}]/\Delta t$ across the interval. Other functions could be used for computing the rate (e.g., MCKIBBEN and BARNES, 1986), but our intervals were short and adequately approximated by finite difference. The rate coefficient was determined by this method only in connection with determining n for A/V. Rate coefficients for other experiments were determined by fitting Eqns. (6) or (8) to the rate data.

RESULTS

The raw time-course data for the experiments reported here are available elsewhere (MOSES, 1988).

Pyrite Surface

The surface areas, as determined by BET measurements, for the unreacted and reacted pyrite grains suggest essentially no change during the experiments (Table 3). The grain-size distributions of the same two samples were also nearly identical (Table 3). There was no evidence of a second mode in the distribution at grain sizes lower than $\bar{D}$.

Table 3. Surface area and grain-size distribution for pyrite grains.

sample	$\bar{A}$[a]	(r)[b]	$\bar{D}$[c]	(se)[d]
unreacted	0.0709	(0.99966)	35.00	(8.51)
reacted	0.0618	(0.99948)	36.69	(9.36)

[a]specific surface area ($m^2 g^{-1}$)
[b]correlation coefficient for 3-point BET isotherm fits for $\bar{A}$
[c]mean of the grain-size distribution (μm)
[d]standard error for $\bar{D}$

Table 4. Model (equation 9) for determination of order with respect to A/V. D.O.-saturated pyrite oxidation experiments at pH 6 and 7 with initial aqueous Fe(II) ranging from 58–82 μM and A/V ratios ranging from 1.65–4.12 $m^2 L^{-1}$.

N[a]	r[b]	n[c]	(se)[d]	log k_n[e]	(se)[d]
52	0.3698	1.01	(0.360)	−3.23	(0.141)

[a]number of data points
[b]correlation coefficient for model
[c]order of reaction (slope of model equation)
[d]standard error for the fitted parameters
[e]log of the rate constant (intercept of model equation); given that $n = 1$, the units of k are μmole pyrite $m^2 s^{-1}$

Equation (9) was fitted to the data from DO-saturated experiments with added Fe(II) to determine the order with respect to A/V (Table 4 and Fig. 2). There is some scatter at pH 7 because we include data here from early experiments when our methods were not fully developed, and some of those experiments yielded lower rates. Scatter may also result from the pH-stat technique. We did not, however, attempt to eliminate those 'outliers,' which seem to bias the computed order ($n_{pH7} = 0.76$). Nevertheless, both the pH 6 data ($n_{pH6} = 1.02$) and the pooled pH 6 and pH 7 data ($n_{pooled} = 1.01$) indicate a reaction order of 1 for A/V.

Oxidation by Dissolved Oxygen

DO-saturated experiments with added initial $Fe(II)_{(aq)}$ were performed at pH 6 and pH 7. Representative time courses are shown in Fig. 3. A particularly striking aspect of these results is the very rapid loss of $Fe(II)_{(aq)}$. Meanwhile, $[Fe(III)_{(aq)}]$ decreases slowly after an initially rapid rate of increase, and $[SO_4^{2-}]$ increases steadily. Rate law parameters for zero-order models (i.e., Eqn. 6) for each pH are given in Table 5 (Fig. 4). The pH 6 rate coefficient, if expressed in μmoles of pyrite, gives a log k of −3.45, and the pH 7 rate coefficient gives a log k of −3.26. The pH 7 data are more scattered than the pH 6 data, principally for the reasons reported above. If, as we suggest, the pH 7 data have been

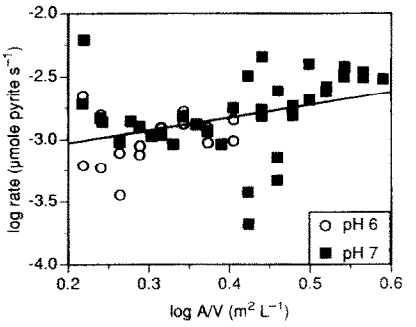

FIG. 2. Model (Eqn. 9) for reaction order with respect to A/V (ratio of pyrite surface area:reaction solution volume). The line is fitted to all data points for DO-saturated experiments at pH 6 and 7 (parameters for the fitted line are given in Table 4).

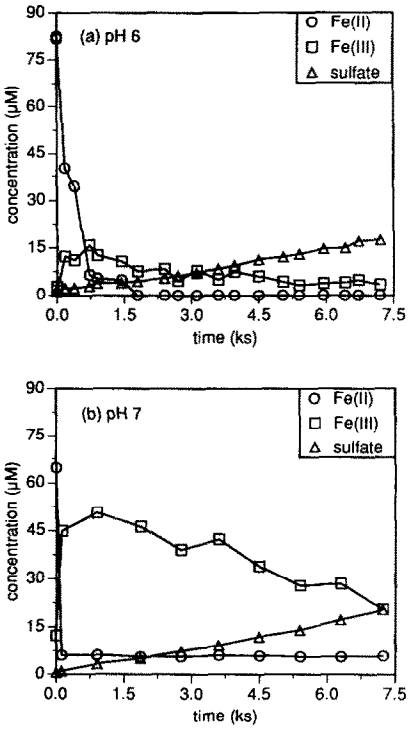

FIG. 3. (a) Representative experimental time course showing concentrations of [Fe(II)], [Fe(III)], and $[SO_4^{2-}]$ at pH 6. (b) Same as (a) except pH 7.

slightly biased to low rates, then actual pH 7 rates are >50% faster than at pH 6. Despite the scatter, uncertainties in k_0 are <10%.

Several DO-saturated experiments were performed at pH 7 without added initial $Fe(II)_{(aq)}$. No $Fe(II)_{(aq)}$ was detected at any time in these experiments. The rate of reaction in the absence of $Fe(II)_{(aq)}$ is significantly greater in the early stages of an experiment than in the later stages (Table 6 and Fig. 5). Note that the 'early stage' ($t \leq 3840$) data were collected from experiments terminated at $t(3840)$, while the 'late stage' ($t \geq 3840$) data were collected from experiments that were initially ~50% saturated with respect to DO. We did not pursue the undersaturated experiments, but used their DO-saturated late stages for comparison with the shorter-duration Fe(II)-free experiments. The undersaturated early stage accounts for the low yield of sulfate at $t(3840)$ compared to the yield of the DO-saturated early stage experiments. The

Table 5. Zero–order rate law parameters for pyrite oxidation with added Fe(II) (equation 6). Data are for D.O.–saturated pyrite experiments at pH 6 and 7. Initial aqueous Fe(II) concentrations ranged from 58–83 μM.

pH	N	r	k_0	(se)
6	20	0.9929	0.351	(0.010)
7	38	0.9361	0.552	(0.035)

Parameters are explained in Table 4. Units of k_0 are nmole pyrite m^2 s^{-1}.

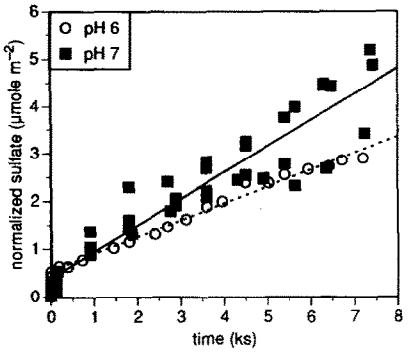

FIG. 4. Sulfate production in DO-saturated solutions at pH 6 (dashed line) and 7 (solid line). The slope of normalized sulfate vs. t gives the rate coefficient for pyrite oxidation according to Eqn. (6). Initial [Fe(II)] in these solutions ranged from 58–83 μM. Parameters for the fitted lines are given in Table 5.

object of comparison, however, is the rate of sulfate production, which is diminished by a factor of ~2 in the late stage data.

Oxidation in the Presence of Fe(III)

The behavior of $[SO_4^{2-}]$ in the anoxic experiments with added initial Fe(III) was similar to that reported by MOSES et al. (1987). A very rapid increase in $[SO_4^{2-}]$ was observed in the first sample interval and was followed by irreproducible changes in concentration (Fig. 6).

The rate of SO_4^{2-} release to solution in the anoxic portion of these experiments can be estimated by comparing the $t(0)$ and $t(120)$ sample concentrations (Table 7). This procedure was followed in earlier work (MOSES et al., 1987), but these estimates can now be corroborated with the Fe(III) analyses of the present study. The rate coefficients for Fe(III) loss, also estimated from the $t(0)$ and $t(120)$ data, can be divided by 14, the number of moles of Fe(III) reduced per mole of pyrite oxidized (reaction 1 and Eqn. 8), to give an estimate of the pyrite oxidation rate that is independent of the estimate obtained with SO_4^{2-} as the RPV (Table 7). The rate coefficients based on [Fe(III)] are larger than those based on $[SO_4^{2-}]$, but only by a factor of 1.5–3 (on average, about 2.2).

It is not possible to quantify the pH-dependent difference in rates with the available data, but the pH 7 rates may be slightly faster. The pH 6 data show that the anoxic reaction

Table 6. Zero–order rate law parameters for pyrite oxidation without added Fe(II) (equation 6). Data are for D.O.–saturated experiments at pH 7.

expt	N	r	k_0	(se)
note a	24	0.9246	1.11	(0.098)
note b	12	0.9596	0.589	(0.055)

[a]samples collected at $t \leq 3840$ s
[b]samples collected at $t \geq 3840$ s
Parameters are explained in Table 4. Units of k_0 are nmole pyrite m^2 s^{-1}. Sulfate concentrations were normalized to constant A/V. Pooling all the data yield $k_0 = 0.674$ ($r = 0.8975$, N = 36)

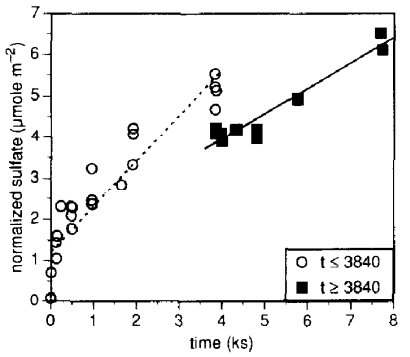

FIG. 5. Sulfate production in DO-saturated solutions at pH 7. No Fe(II) was added to these solutions, and none was detected during the experiments. Two groups of samples are shown ($t \leq 3840$ s, dashed line, and $t \geq 3840$ s, solid line) for comparison of sulfate production rates in early and late stages of an experiment. Parameters for the fitted lines are given in Table 6.

is dependent on $[Fe(III)_{(aq)}]$, but we do not have sufficient data to determine the order of the reaction.

After the O_2 purge gas was started at the midpoint of the Fe(III) experiments, $[SO_4^{2-}]$ increased monotonically and reproducibly (Fig. 6; Table 8). No dependence on either pH or $[Fe(III)_{(aq)}]$ could be detected in the rates of reaction in these experiments.

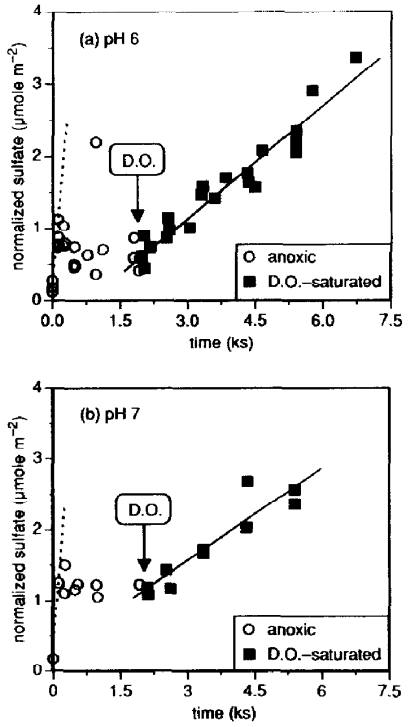

FIG. 6. (a) Sulfate production in solutions with Fe(III) at pH 6. The solutions were initially anoxic and were brought to DO-saturation at the time indicated by the arrow. The dashed line indicates the rate of sulfate production very early in the anoxic stage of the experiment. Parameters for the fitted solid line are given in Table 8. (b) Same as (a) except pH 7.

Table 7. Estimated zero-order rate constants for pyrite oxidation experiments with initial Fe(III). Data are from anoxic pH 6 and 7 experiments. Independent estimates were obtained from Fe(III) and SO_4^{2-} concentrations (normalized to A/V) at t(0) and t(120).[a]

pH	[Fe(III)][b]	$k_{0,S}$[c]	k_F[d]	$k_{0,F}$[e]
6	104	6.40	−235	16.8
6	103	7.65	−244	17.4
6	68	4.85	−163	11.6
6	67	4.65	−197	14.0
7[f]	73	5.80	−121	8.6
7	72	9.55	−189	13.5

[a]The estimates in this table are slopes between these first 2 data points, so no descriptive statistics could be computed.
[b]initial concentration (μM)
[c]zero-order rate constant for pyrite oxidation based on sulfate accumulation (equation 6)
[d]zero-order rate constant for loss of Fe(III)
[e]zero-order rate constant for pyrite oxidation based on Fe(III) loss (equation 6); units of $k_{0,S}$ and $k_{0,F}$ are nmole pyrite m^2 s^{-1}
[f]rate based on sulfate determined from data at t(260) seconds because both t(0) and t(120) samples were lost before analysis; the t(0) concentration was assumed to be zero

DISCUSSION

Reaction Progress Variables

The experiments in this study differ from previous pyrite oxidation experiments in the direct measurement of aqueous Fe(II) and Fe(III) during the time course. As these experiments were begun, we planned to use $Fe(II)_{(aq)}$ as the RPV. In other words, accumulation of $Fe(II)_{(aq)}$ would be equated to pyrite dissolution in a manner consistent with reactions (1) and (2). A potential difficulty with Fe(II) as an RPV was anticipated, namely its oxidation in the presence of DO. We had planned to account for this by carefully modeling the oxidation of $Fe(II)_{(aq)}$ in identical experiments without pyrite (MOSES and HERMAN, 1989). This plan was foiled by the extent to which Fe(II) was removed from solution (see below), and after a number of experiments were performed in which $[Fe(II)_{(aq)}]$ could barely be measured, it was concluded that SO_4^{2-} analyses were, in fact, required.

Aqueous sulfur has been shown, however, to be a difficult RPV (GOLDHABER, 1983; MOSES et al., 1987; see also discussions in MCKIBBEN, 1984, and MCKIBBEN and BARNES, 1986). One potential difficulty is the involvement of inter-

Table 8. Zero-order rate constants for pyrite oxidation experiments with initial Fe(III) (equation 6). Data are from D.O.-saturated pH 6 and 7 experiments.

pH	N	r	k_0	(se)
6	21	0.9628	0.512	(0.033)
7	10	0.9305	0.438	(0.061)
6 and 7	31	0.9265	0.483	(0.036)

Parameters are explained in Table 4. Units of k_0 are nmole pyrite m^2 s^{-1}.

mediate sulfoxy species, such as thiosulfate and the polythionates, in the oxidation of pyrite S. Such species can, under some circumstances, accumulate in the reaction solution where they are oxidized homogeneously. Under these circumstances, the rate of accumulation of sulfate would not necessarily reflect the rate of pyrite oxidation, and the stoichiometric relationships assumed in developing rate expressions like Eqn. (4) would be invalidated. The only suitable RPV would then be ΣS (total sulfur). In this study, we did not analyze or consider intermediate sulfoxy anions in our rate-law development nor did we use ΣS as an RPV. Our use of sulfate as an RPV is justified by the data of MOSES et al. (1987), which show negligible accumulation of sulfoxy intermediates under the conditions of our present experiments. For example, at pH 7 in a DO-saturated experiment, the rates of thiosulfate and polythionate accumulation over 24 h were <5% of the sulfate accumulation rate. More importantly, no intermediates were observed at times less than 4 h into the experiment. Therefore, in the DO-saturated experiments of this study (all ≤7440 *s* in duration), we are confident that $\Sigma S = [SO_4^{2-}]$, validating both the stoichiometry of reactions (1) and (2) and the form of Eqn. (4). NICHOLSON et al. (1988) detected <5% nonsulfate S in their circumneutral-pH systems and similarly assumed $\Sigma S = [SO_4^{2-}]$. Furthermore, in the anoxic Fe(III) experiments of MOSES et al. (1987), sulfoxy intermediates were never detected, so we are confident that $\Sigma S = [SO_4^{2-}]$ in those experiments as well.

There remains a second potential difficulty with any form of sulfur as RPV. The pyrite surface plays a fundamental role in pyrite oxidation. Adsorption of Fe(II) was demonstrated by this study, and earlier studies showed that, under certain conditions, pyrite appears to adsorb SO_4^{2-} (GOLDHABER, 1983; MOSES et al., 1987). The full range of the behavior of pyrite as an adsorbent is still unknown, so there remains room for doubt that dissolved sulfur accumulation rates are directly related to pyrite oxidation rates. Accordingly, in the discussion of the pyrite oxidation results of this study, it will be understood that the reported rate coefficients are tentative.

Note that the rate coefficients can depend on RPV. Those based on SO_4^{2-} accumulation during anoxic pyrite oxidation by Fe(III) are lower by a factor of 1.5 to 3 than those based on Fe(III) loss (Table 7). Loss of Fe(III) due to reduction by pyrite, however, was compounded by Fe(III) loss due to precipitation of oxyhydroxides. The sampling method was designed to collect these solids, but in practice some Fe(III)-oxyhydroxides were trapped on the screen that covered the sampling pipet, so observed Fe(III) concentrations were slight underestimates of the quantity $\Sigma[Fe(III)] = [Fe(III)_{(aq)}] + [Fe(III)_{(s)}]$. We noted that the oxyhydroxides did not appear to be lost on the pyrite surface. We have observed in slowly stirred, long-duration pyrite-oxidation systems at circumneutral pH that the pyrite surface may take on a 'rusty' appearance attributable to the deposition of Fe(III)-oxyhydroxides on the surface. In the well-stirred and short-duration experiments of this study, the bright lustre of the pyrite surface was undiminished over the time course. Nevertheless, because our observed $\Sigma[Fe(III)]$ was a slight underestimate of the actual $\Sigma[Fe(III)]$, the Fe(III)-based rates are slight overestimates of the pyrite dissolution rates. Some loss of SO_4^{2-} is also suggested by the data (Fig. 6), so the sulfate-based rates are probably slight underestimates of the pyrite dissolution rates. The rate coefficients for pyrite oxidation by Fe(III) in anoxic solutions are, thus, constrained to the 5–15 nmole pyrite $m^2\ s^{-1}$ range.

Our experiments did not employ a wide range of $Fe(III)_{(aq)}$ concentrations, which made it impossible for us to test our assumption that the dependence of the oxidation reaction on $[Fe(III)_{(aq)}]$ is zero-order (Eqn. 5). In fact, our data indicate that the dependence is not zero-order (Table 7). MCKIBBEN and BARNES (1986) report a square-root dependence on Fe(III) at low pH where Fe^{3+} is the dominant species. At higher pHs, Fe(III) hydrolysis may influence the nature of the dependence on Fe(III), so a greater range of $[Fe(III)_{(aq)}]$ will need to be used in subsequent experiments along with pH-dependent Fe(III) speciation modeling to determine the order of pyrite oxidation with respect to Fe(III). Once this is done, the rate coefficients we report in Table 7 will have to be revised to reflect the modification of the rate law.

The Pyrite Surface

During an experiment, some decrepitation (or comminution) of the pyrite grains was expected, which would have increased the number of particles with smaller grain size at the expense of larger particles and, thus, yielded a larger specific surface area. We observed, however, that $\bar{A}$ decreased slightly during the reaction, although the uncertainty in the measurement prevents one from ruling out $\Delta\bar{A} = 0$ (Table 3). The mean grain sizes for the two samples were also not statistically different (Table 3). Note that the standard deviation for $\bar{D}$ is relatively large because the distribution fits a rather broad bell-shaped curve. Nevertheless, the before-experiment and after-experiment distributions are nearly identical. We conclude, on the basis of both $\bar{A}$ and $\bar{D}$, that $\Delta\bar{A}$ was negligible. This conclusion has been reached by other workers using this type of experimental system (J. D. Rimstidt, pers. comm., 1987). The lack of any mode in the grain-size distribution at lower sizes increases confidence that fines were removed adequately during the cleaning procedure and that none were created during experiments. In our experiments, the lack of decrepitation may be explained by the stirring method employed by our apparatus. Instead of a stir-bar or impeller that would impact or grind the grains, the titration assembly uses a rod rotated rapidly on its longitudinal axis creating a vortex in the reaction solution. Our finding of no surface area change validates the procedure we adopted for normalizing concentrations to A/V, which, because surface area was constant, was merely a correction for the volume decrease as samples were removed from the reaction solution.

Our finding of unit reaction order with respect to A/V is consistent with other reports (e.g., MCKIBBEN and BARNES, 1986; NICHOLSON et al., 1988). We share the concerns of MCKIBBEN and BARNES (1986) regarding the potential differences between BET surface area and reactive surface area. So far, however, no pyrite oxidation study has detected any departure from a straightforward proportionality between BET surface area and rate. On the other hand, the duration

of pyrite oxidation experiments may not have been long enough to detect any such departure. Pyrite oxidation studies have also not addressed the issues raised by HOLDREN and SPEYER (1985) concerning grain size and defect density.

Adsorption of Fe by Pyrite

Anoxic oxidation by Fe(III), while very fast, could not be sustained for more than a few minutes (Fig. 6). The early cessation of oxidation was enigmatic because there was still a considerable amount of Fe(III) remaining in solution. Based on the stoichiometry (reaction 1), the reduction of Fe(III) on pyrite would produce 7.5 times as much Fe(II) as SO_4^{2-}, but because $Fe(II)_{(aq)}$ was only observed in very small concentrations ($\ll[SO_4^{2-}]$), we began to suspect that it was adsorbing to the pyrite surface where it evaded our aqueous sampling. We inferred that the oxidation reaction was halted by the adsorption of Fe(II), which blocked the reactive surface sites to which Fe(III) needed access. We discuss below why Fe(II) adsorption should be preferred to that of Fe(III).

A related observation from the DO-saturated experiments that included $Fe(II)_{(aq)}$ at $t(0)$ was the rapid loss of Fe(II) from solution. In these experiments, the rate of loss of Fe(II) greatly exceeded the rate of loss due to oxidation alone (Fig. 7). The oxidation rate of Fe(II) under identical conditions, except for the absence of pyrite, was reported by MOSES and HERMAN (1989) and was used here to predict the loss of Fe(II) by oxidation alone. It is known that Fe(II) oxidation can be catalyzed by adsorption on oxide surfaces (summary in WEHRLI and STUMM, 1989), but in our experiments, the increase in [Fe(III)] accounted for only a fraction of the lost Fe(II) in the presence of pyrite (Fig. 3). While the catalysis of Fe(II) oxidation by sulfide surfaces should be examined, the most straightforward explanation of our results is that Fe(II) was removed from solution by adsorption onto the pyrite surface.

There was no evidence of Fe(III) adsorption to the pyrite surface. There are at least two reasons to expect Fe(II) adsorption but little or no Fe(III) adsorption. First, at pH 6 or 7, Fe(II) is present almost solely as Fe^{2+}, while Fe(III) is present as $Fe(OH)_2^+$ (99% at pH 6 and ~90% at pH 7) or $Fe(OH)_3^0$ (~10% at pH 7). To the extent that the adsorption is electrostatic, then, Fe(II) adsorption should be greater. This assumes that the pyrite surface charge is negative, so that cations can adsorb electrostatically. In the context of these experiments, this would require a $pH_{zpc} < 6$. GOLDHABER (1983) suggested that $pH_{zpc,\ pyrite}$ is ~7.3, based on the acidity of H_2S_2. However, if one considers the series of sulfane acids H_2S_n, the pK_{a1} decreases with increasing n, as is the case with the silica acids. If this sequence could be extrapolated to infinite n, as in a crystalline disulfide, one might predict that $pH_{zpc,\ pyrite}$ is as low as 1–3, as is that for quartz (J. D. Rimstidt and J. B. Murowchick, pers. comm., 1987). This speculative argument has recently been corroborated by microelectrophoretic measurements, which show that $pH_{zpc,\ pyrite} = 2.5$ (C. P. Huang, pers. comm., 1989).

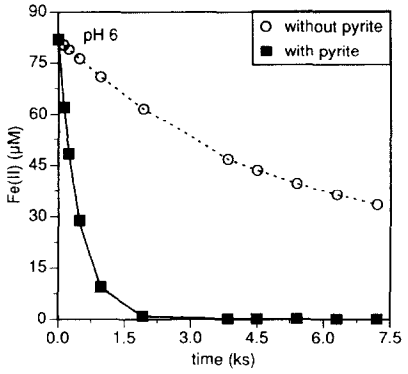

FIG. 7. Loss of Fe(II) in DO-saturated solutions at pH 6. Points on the plot are model results. The rate law for modeling the loss of Fe(II) by oxidation alone (without pyrite, dashed line) is given in MOSES and HERMAN (1989). The rate law for modeling the loss of Fe(II) in the presence of pyrite (solid line) was derived by fitting [Fe(II)] data such as that shown in Fig. 2(a) to an equation of the form $\frac{-d[Fe(II)]}{dt} = k[Fe(II)]^n$. A model similar to Eqn. (9) was used to determine $\log k = -3.373$ and $n = 1.356$ ($r = 0.9698$).

A low pH_{zpc} means that, for the systems studied here and, in fact, for most previous studies and in most natural waters, the surface charge of pyrite is negative and is independent of pH. Because the surface charge is pH independent, adsorption processes are good candidates for any pH-independent interference with oxidative attack by Fe(III). The pH independence of the charge on Fe(II) at $pH < 8.5$ is consistent with the notion that it may be the interfering adsorbate. The pH-dependent speciation of Fe(III), on the other hand, raises the question of whether it may become a more important adsorbate on the pyrite surface at lower pHs.

Second, the adsorption may be more selective than simple electrostatic attraction. The basis for this is the principle of hard and soft acids and bases (HSAB), a useful rule-of-thumb for predicting the relative stability of Lewis acid-base complexes. According to HSAB, hard acids preferentially complex with hard bases, and soft acids preferentially complex with soft bases. Disulfide is a soft base, and while Fe(III) is not especially hard, Fe(II) is softer (HUHEEY, 1972). A bond between the disulfide-dominated pyrite surface and Fe(II) is, therefore, preferred to one between the surface and Fe(III).

We would not expect, on the basis of HSAB or any theory, that a bond between Fe(III) and the pyrite surface would be forbidden. In fact, such a bond must take place, at least in a transition state, for the two to react. LUTHER (1987) proposed, on the basis of molecular orbital theory and symmetry arguments, that Fe(III) loses one H_2O ligand and binds as a Lewis acid with the Lewis base pyrite surface. The disulfide component of pyrite acts as the bridging (persulfido) ligand between the Fe(II) of pyrite and the adsorbed Fe(III) (see TAUBE, 1984, for a discussion of inner-sphere electron-transfer reactions between two metals bound by a bridging ligand). The Fe(III) may not be able to eject the softer and preferred Fe(II) from a soft base surface site, but it should be preferred to harder acids like H^+, Li^+, or Na^+ (the other cations present in our reaction solutions).

Mechanism of Pyrite Oxidation at Circumneutral pH

The relative rate coefficients for pyrite oxidation under the different experimental conditions of this study are summarized in Table 9. The anoxic oxidation by Fe(III), at either pH 6 or pH 7, gave the fastest rates by far of all the experi-

Table 9. Rough comparison of the rates of pyrite oxidation at circumneutral pH.

conditions	approximate k_0[a]	
anoxic, with Fe(III)	10	(<120 s)[b]
oxic, no initial Fe	1	(≤3840 s)
oxic, no initial Fe	0.5	(≥3840 s)
oxic, with initial Fe(II) or Fe(III)	0.5	
anoxic, with Fe(III)	0	(>120 s)

[a]Units of k_0 are nmole pyrite m^2 s^{-1}.
[b]Number in parentheses gives period of experiment for which approximate k_0 is valid.

mental oxidants (Table 7). These fast rates only lasted a few minutes into the experimental time course, after which the rate dropped to zero (Fig. 6).

The data from the DO-saturated experiments without added $Fe(II)_{(aq)}$ were divided into a group of samples collected prior to $t(3840)$ and a group of samples collected after $t(3840)$ for the purpose of comparing the early stages of an experiment to the later stages (Table 6 and Fig. 5). As explained above, these samples were gathered from two separate sets of experiments that differed only in the level of DO saturation at $t < 3840$; only the DO-saturated portions of the experiments are compared here. All of these experiments began with no Fe(II) added to the reaction solution. We found that the early stage gave the second-fastest pyrite oxidation rates observed in this study (Table 6). In the later stages, however, the rates were slower—essentially the same as those observed throughout an experiment with added $Fe(II)_{(aq)}$ (compare Tables 5 and 6). This evidence suggests that DO can attack pyrite, but the accumulation of adsorbed Fe during the early stage interferes with this reaction, as indicated by the diminished late-stage rate of oxidation. Oxidation of pyrite by DO produces only $^1/_5$ the amount of Fe(II) produced by oxidation by Fe(III) (cf. reactions 1 and 2), so it can be sustained longer before Fe(II) accumulates on the surface to a point that it begins to interfere with the direct reaction with DO.

Several authors have proposed rate laws, rate coefficients, and reaction mechanisms involving direct attack by DO on the pyrite surface (e.g., GOLDHABER, 1983; MCKIBBEN and BARNES, 1986; NICHOLSON et al., 1988). Experimentally testing such models is complicated by the release of Fe by the reaction under examination. Once Fe is present with DO, Fe(III) will be generated (quite rapidly at circumneutral pH). Furthermore, our results indicate that Fe(II) can accumulate on the pyrite surface with time, interfering with direct attack by DO. Accordingly, rate data for examining the reaction between DO and pyrite must be collected very early in the time course. Despite experimental artifacts that prevented their use of the initial rates method in handling their rate data (which contributed considerably to the success of the MCKIBBEN and BARNES, 1986, experiments), NICHOLSON et al. (1988) did deduce a useful adsorption model for DO on pyrite. According to their model, high DO concentrations lead to pseudo zero-order rate behavior (which we assumed in our rate law development), low concentrations lead to pseudo first-order behavior, and intermediate concentrations give orders between 0 and 1. The credibility of this model is not affected by their data handling procedures, but now that we have evidence that Fe(II) and DO compete for surface sites, experiments can be designed to carefully test the NICHOLSON et al. (1988) model with the initial rates method.

Other than the zero rate of oxidation after a short initial rapid rate in anoxic Fe(III) solutions, we observed the slowest rates during oxidation by DO when aqueous Fe was present, whether during an experiment with initial $Fe(II)_{(aq)}$ (Table 5), in the later stages of an experiment with no initial Fe (Table 6), or in the later stages of an experiment with initial Fe(III) (Table 8). The decreased rate of oxidation in these experiments parallels the evidence for Fe(II) adsorption on the pyrite surface, so we attribute the decreased rate to the accumulation of Fe(II) on the surface, whether the Fe(II) was initially present or accumulated during pyrite oxidation. These slowest rates, obtained in the presence of DO after Fe(II) accumulation had reduced the rate, could be sustained for the duration of any of the experiments.

Our comparison of rates suggests that Fe(III) is more reactive with pyrite than DO is. MOSES et al. (1987) argued that DO was an unlikely oxidant of pyrite because it is paramagnetic, while pyrite is diamagnetic. The reaction between the two would be spin restricted and very unlikely. Adsorbed oxygen could, however, be activated to a diamagnetic electronic configuration, and LUTHER (1987) suggested that DO can, in fact, react with pyrite, but only slowly. The proposed mechanism of LUTHER (1987; based on molecular orbital theory) for pyrite oxidation by DO is more consistent with the new experimental data than the rejection of a DO-pyrite reaction by MOSES et al. (1987). Our evidence shows that pyrite can react with DO, albeit more slowly than with Fe(III), confirming the prediction of LUTHER (1987).

Equation (10) shows, in schematic form, an encounter between Fe(III) and a reduced (electron-rich, anodic) site on the pyrite surface and the formation of a transition state that could decompose to yield the original unbound reactants or the product, namely Fe(II) bound to a partially-oxidized site.

$$\text{Fe(III)} + \text{pyrite}_{red} \rightleftarrows \text{Fe(III)-pyrite}_{red} \rightarrow \text{Fe(II)-pyrite}_{ox} \quad (10)$$

The redox-potential difference accounts for the direction of electron transfer. Potential differences account for the relative irreversibility of the forward decomposition of the transition state. Even though the Fe(II) is bound to a relatively oxidized site in the $Fe(II)\text{-pyrite}_{ox}$ product, the electron reservoir in the bulk pyrite is so large that electron transfer from Fe(II) to pyrite (reversal of the second step of equation (10)) is unlikely.

The origin of the transition state ($Fe(III)\text{-pyrite}_{red}$) in reaction (10) is the oxidation of an adsorbed Fe(II) (Eqn. 11):

$$\text{Fe(II)} + \text{pyrite}_{red} \rightleftarrows \text{Fe(II)-pyrite}_{red} \xrightarrow{DO} \text{Fe(III)-pyrite}_{red} \rightarrow \text{Fe(II)-pyrite}_{ox}. \quad (11)$$

This reaction is the basis of the cyclic mechanism that we propose below. It differs from reaction (10) in that the initial

adsorbate is Fe(II), which the evidence shows to be the preferred form. The adsorption of Fe(II) then requires an additional oxidation step before the oxidation of the pyrite. The oxidation of the adsorbed Fe(II) is unidirectional because H_2O (the product of DO reduction) will not reduce Fe(III). The last step, in which the pyrite is oxidized and the Fe(III) reduced, must take place faster than the dissociation of the Fe(III)-pyrite$_{red}$ complex (i.e., loss of Fe(III) to the solution; not shown). This step is also unidirectional, as in reaction (10), owing to the redox-potential gradient. As long as the pyrite$_{ox}$ form is less oxidized than the form that dissociates from the surface (probably thiosulfate or a more oxidized form), the Fe(II)-pyrite$_{ox}$ complex is cycled back to the Fe(II)-pyrite$_{red}$ form for further oxidation.

The pyrite$_{ox}$ species of reactions (10) and (11) dissociates from the surface when the sulfoxy species is more stable in solution than remaining at the surface. A number of studies suggest that it is the Fe-S bond that weakens during oxidation rather than the S-S bond in the disulfide (GOLDHABER 1983; MCKIBBEN and BARNES, 1986; LUTHER, 1987; MOSES et al., 1987). MOSES et al. (1987) showed that the relative stability of intermediate sulfoxy species was pH dependent and that very vigorous stirring of the reaction solution was required before they could be observed in solution at all. Apparently, oxidation of sulfoxy species from pyrite S to sulfate generally takes place either at the surface or in a near-surface region of the solution, and the intermediates can be observed in bulk solution when the near-surface region is disrupted by substantial turbulence. Even with vigorous stirring, they are not observed until well into the experimental time course, which justifies the use of sulfate as RPV in the present experiments. The intermediates may also be observed when conditions are less oxidizing than in our experiments (e. g., GRANGER and WARREN, 1969; BOULEGUE, 1979), but we do not have data to address this possibility.

Extending the Singer-Stumm Model

The work completed in this study leads to the conclusion that the Singer-Stumm model of pyrite oxidation (SINGER and STUMM, 1970a) applies to any pH. This study showed that, although DO can directly oxidize pyrite, it can effectively do so only in the absence of Fe(II) adsorbed to the pyrite surface. Iron(III) is the preferred direct oxidant, oxidizing pyrite very rapidly but, as with DO, only in the absence of adsorbed Fe(II). In natural systems, however, Fe(II) will always be present to interfere with pyrite oxidation by either DO or Fe(III) and will thereby limit the rate at which pyrite oxidation can be sustained. What is needed is a mechanism for pyrite oxidation that explains how the process can be sustained once the reactive surface sites are occupied by adsorbed Fe(II). Any proposed mechanism must take into account the evidence for adsorbed Fe(II) and the decreases in oxidation rate observed when the reaction is initiated without added Fe(II), and it must show how pyrite oxidation can continue for more than a short period of time.

When Fe(II) is adsorbed to the surface, the likely situation during pyrite oxidation in natural waters, oxidation appears to involve the transfer of electrons from pyrite to DO via the adsorbed Fe, which is cyclically oxidized to Fe(III) (the preferred oxidant) by DO and becomes Fe(II) again (the preferred adsorbate) upon taking up another electron from the pyrite (reaction 11; Fig. 8). The results of Fe(II) oxidation experiments reported elsewhere (MOSES and HERMAN, 1989) support a termolecular reaction complex with two Fe(II) molecules for each DO molecule, and we have assumed that this configuration applies to the adsorbed Fe(II) as well. The question of the kinetics of oxidation of adsorbed Fe(II) is certainly an open question, however, both in terms of rate and mechanism. The process depicted in Fig. 8 continues with intermediate rehydration of the adsorbed Fe until some sulfoxy species dissociates from the surface.

The roles for DO and Fe(III) in pyrite oxidation, thus, have much less to do with which is the more important direct oxidant than with how they are both involved in the oxidation of pyrite when its surface sites are occupied by adsorbed Fe. Adsorbed Fe(III) still is the species that accepts electrons from the pyrite (the unidirectional part of reaction 10 and step b in Fig. 8). The relatively reduced Fe(III)-pyrite$_{red}$ species (the transition state) is regenerated by oxidation of the adsorbed Fe(II) in the partially oxidized Fe(II)-pyrite$_{ox}$ species (Fig. 9). The pyrite$_{ox}$ can dissociate from the surface, if the sulfur moiety is oxidized enough to be a stable sulfoxy anion in solution, but if not, it is still reduced with respect to Fe(III) and participates as Fe(III)-pyrite$_{red}$ on the next cycle.

We consider our model an extension of the Singer-Stumm model because the rate-limiting step is still the oxidation of Fe(II). The original concept of the Singer-Stumm model applied to low pH where Fe(II) oxidation is rate-limiting because it is slower than the rate at which Fe(III) can oxidize pyrite. The true rate-limiting step for pyrite oxidation by Fe(III) at circumneutral pH may be the formation of the first S-O bond (the transfer of oxygen to pyrite S from the Fe(III) hydration

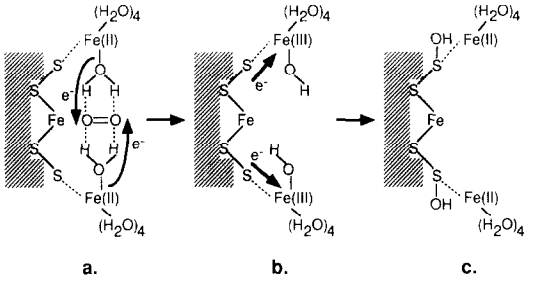

FIG. 8. Schematic sequence of reaction steps for the oxidation of pyrite sulfur. (a) Adsorbed Fe(II) (preferred over Fe(III) as an adsorbate) forms a hydrogen-bonded termolecular complex with DO, and electrons are transferred from Fe(II) to DO. The product of DO reduction is not shown (see MOSES and HERMAN, 1989). One of the 6 waters of hydration on the aquo-Fe complex has been lost to accommodate the bond for the Lewis acid-base surface complex. (b) Electrons are transferred rapidly from pyrite to the adsorbed Fe(III) that results from step (a). The adsorbed Fe(III) is unstable both with respect to reduction by pyrite and with respect to displacement by a softer Lewis acid, such as Fe(II), but its reduction is so rapid that displacement is an unlikely fate. (c) An OH group has been transferred from the adsorbed aquo-Fe(III) in response to the electron transfer shown in step (b). The adsorbed Fe species is now Fe(II), which is the more stable adsorbate but is unstable with respect to oxidation by DO. After rehydration, the Fe(II) in step (c) can be oxidized again as in step (a), and so on.

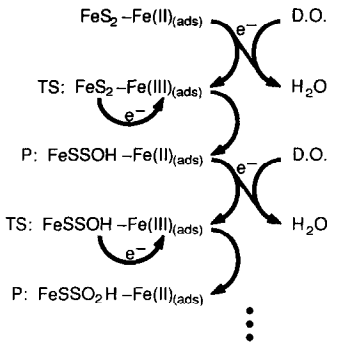

FIG. 9. Schematic reaction sequence, emphasizing the redox cycle undergone by the adsorbed Fe. DO never directly reacts with the pyrite, but its reduction drives the oxidation of pyrite by generating reactive Fe(III) directly on the pyrite surface. The electrons transferred from pyrite to the adsorbed Fe(III) are ultimately transferred to DO when the adsorbed Fe(II) is oxidized. TS (transition state) corresponds to Fe(III)-pyrite$_{red}$ in reactions (10) or (11), while P (product) corresponds to Fe(II)-pyrite$_{ox}$. The product of one step in the cycle is the starting point for the next step. The implied chemical reactions are illustrative but are not balanced in detail.

sphere), as suggested by BIEGLER and SWIFT (1979), MOSES et al. (1987), and LUTHER (1987). In practical terms, however, the maximum rate of pyrite oxidation as limited by this step cannot be sustained when Fe(II) adsorbs to and blocks the reaction sites. Similarly, the maximum rate of pyrite oxidation by DO may be limited by the attachment of O to S or the desorption of products, as suggested by MCKIBBEN and BARNES (1986) and by NICHOLSON et al. (1988), but in either case, it cannot be sustained in the presence of adsorbed Fe(II). The slow but sustainable pyrite oxidation mechanism that is most important in natural waters of low or circumneutral pH is limited by the rate at which DO can oxidize adsorbed Fe(II).

CONCLUSIONS

The rate of pyrite oxidation at circumneutral pH was found to be first-order with respect to A/V. The reaction was accompanied by adsorption of Fe(II) from the reaction solution. The adsorbed Fe(II) apparently blocked the surface reaction sites at which either Fe(III) or DO would oxidize the pyrite because the oxidation rates slowed when Fe(II) accumulated on the surface. Although Fe(III) is evidently the preferred reactant, the reaction could only be sustained in the presence of DO. Therefore, the proposed reaction mechanism involves electron transfer from adsorbed Fe(II) to DO followed by electron transfer from pyrite to the resulting adsorbed Fe(III). Oxygen added to pyrite S comes from water in the hydration sphere of the adsorbed Fe, and the adsorbed Fe cycles between +II and +III oxidation states, alternately accepting an electron from pyrite and passing an electron to DO.

This mechanism extends the Singer-Stumm model for pyrite oxidation, which states that Fe(II) oxidation limits the rate of pyrite oxidation at low pH. The extended Singer-Stumm model now states that the oxidation of Fe(II) limits the rate of pyrite oxidation at low and circumneutral pH. Fe(II) oxidation is rate limiting at low pH because it is much slower than the oxidation of pyrite by Fe(III)$_{(aq)}$. At circumneutral pH, Fe(II) oxidation is rate limiting because Fe(II) adsorbs to the pyrite surface and blocks attack by Fe(III)$_{(aq)}$ or DO. The adsorbed Fe(II) must be oxidized by DO to generate Fe(III) at the pyrite surface.

One topic for future work that deserves special attention is the need to develop relationships between understanding of these processes in simple systems, such as those of this study, and in natural systems. Natural systems are more complicated in terms of solution and solid phase compositions and the activity of biota (mainly bacteria) that may alter the rate or mechanism of the reactions. The proposed pyrite oxidation mechanism of this study is, in fact, compatible with our understanding of the means by which thiobacilli accelerate pyrite oxidation, namely by accelerating the rate of Fe(II) oxidation. What is missing, however, are the links between the molecular-level abiotic mechanism proposed here and the physiological processes that support bacterial life.

Acknowledgments—This research was funded by the National Science Foundation through grants EAR-8418150 and EAR-8417122 (awarded to JSH), the Jeffress Foundation (awarded to JSH), and a Moore Research Award (to COM). Additional funding was provided to COM by the University of Virginia and Lehigh University. We are grateful for the surface area analyses provided by J. D. Rimstidt, the grain-size determinations provided by A. Meglis, the spectrographic pyrite analysis provided by N. Suhr, permission to quote a report on electrokinetic investigations of sulfide minerals provided by C. P. Huang, and laboratory assistance provided by C. M. Wicks. We appreciate helpful and influential discussions with several colleagues, including G. M. Hornberger, C. P. Huang, G. W. Luther, III, M. A. McKibben, A. L. Mills, J. B. Murowchik, D. K. Nordstrom, J. D. Rimstidt, and D. C. Thorstenson. Two anonymous reviews and reviews by M. A. McKibben and J. D. Rimstidt helped us improve the original manuscript.

Editorial handling: T. Pačes

REFERENCES

APHA (1976) *Standard Methods for the Examination of Water and Wastewater*, 14th edn. American Public Health Association.

BERNER E. K. and BERNER R. A. (1987) *The Global Water Cycle.* Prentice-Hall.

BERNER R. A., LASAGA A. C., and GARRELS R. M. (1983) The carbonate-silicate cycle and its effect on atmospheric carbon dioxide over the past 100 million years. *Amer. J. Sci.* **283,** 641–683.

BIEGLER T. and SWIFT D. A. (1979) Anodic behavior of pyrite in acid solutions. *Electrochim. Acta* **24,** 415–426.

BOULEGUE J. (1979) Formation des eaux thermales sulfurées des Pyrénées Orientales. *J. Fran. Hydrol.* **10,** 91–102.

BRUNAUER S., EMMETT P. H., and TELLER E. (1938) The adsorption of gases in multimolecular layers. *J. Amer. Chem. Soc.* **60,** 309–319.

CARUCCIO F. T. (1975) Estimating the acid potential of coal mine refuse. In *The Ecology of Resource Degradation and Renewal* (eds. M. J. CHADWICK and G. T. GOODMAN), pp. 197–205. Blackwell Scientific Publishers.

CHANTRET F. and BOULEGUE J. (1980) Mise en évidence de soufre élémentaire et de sidérite dans des gisements d'uranium de type "roll". *C. R. Acad. Sci. Paris* **290,** D73-D76.

CLARK C. S. (1966) Oxidation of coal mine pyrite. *J. Sanit. Eng. Div. Amer. Soc. Civ. Eng.* **92,** 127–145.

GARRELS R. M. and THOMPSON M. E. (1960) Oxidation of pyrite by iron sulfate solutions. *Amer. J. Sci.* **258-A,** 57–67.

GOLDHABER M. B. (1983) Experimental study of metastable sulfur oxyanion formation during pyrite oxidation at pH 6-9 and 30°C. *Amer. J. Sci.* **238,** 193–217.

GRANGER H. C. and WARREN C. G. (1969) Unstable sulfur compounds and the origin of roll-type uranium deposits. *Econ. Geol.* **64**, 160–171.

HERLIHY A. T., MILLS A. L., and HERMAN J. S. (1988) Distribution of reduced inorganic sulfur compounds in lake sediments receiving acid mine drainage. *Appl. Geochem.* **3**, 333–344.

HISKEY J. B. and SCHLITT W. J. (1982) Aqueous oxidation of pyrite. In *Interfacing Technologies in Solution Mining; Proc. 2nd SME-SPE Internatl. Soln. Mining Conf.* (eds. W. J. SCHLITT and J. B. HISKEY), pp. 55–74.

HOLDREN G. R., JR. and SPEYER P. M. (1985) Reaction rate-surface area relationships during the early stages of weathering. *Geochim. Cosmochim. Acta* **49**, 675–681.

HOLLAND H. D. (1978) *The Chemistry of the Atmosphere and Oceans.* Wiley-Interscience.

HOLLAND H. D. (1984) *The Chemical Evolution of the Atmosphere and Oceans.* Princeton University Press.

HUHEEY J. E. (1972) *Inorganic Chemistry.* Harper and Row.

KLEINMANN R. L. P. and CRERAR D. A. (1979) *Thiobacillus ferrooxidans* and the formation of acidity in simulated coal mine environments. *Geomicrobiol. J.* **1**, 373–388.

LASAGA A. C. (1981) Rate laws of chemical reactions. In *Kinetics of Geochemical Processes* (eds. A. C. LASAGA and R. J. KIRKPATRICK); *Reviews in Mineralogy* **8**, pp. 1–68.

LOWSON R. T. (1982) Aqueous oxidation of pyrite by molecular oxygen. *Chem. Rev.* **82**, 461–497.

LUTHER G. W., III (1987) Pyrite oxidation and reduction: Molecular orbital theory considerations. *Geochim. Cosmochim. Acta* **51**, 3193–3199.

MASON B. (1966) *Principles of Geochemistry*, 3rd edn. Wiley.

MCKIBBEN M. A. (1984) Kinetics of aqueous oxidation of pyrite by ferric iron, oxygen and hydrogen peroxide from pH 1-4 and 20-40°C. Ph.D. dissertation, Pennsylvania State University.

MCKIBBEN M. A. and BARNES H. L. (1986) Oxidation of pyrite in low temperature acidic solutions: Rate laws and surface textures. *Geochim. Cosmochim. Acta* **50**, 1509–1520.

MOSES C. O. (1988) Oxidation of ferrous iron and pyrite at circumneutral pH. Ph.D. dissertation, University of Virginia.

MOSES C. O., HERLIHY A. H., HERMAN J. S., and MILLS A. L. (1988) Ion chromatographic analysis of mixtures of ferrous and ferric iron. *Talanta* **35**, 15–22.

MOSES C. O. and HERMAN J. S. (1989) Oxidation of ferrous iron at circumneutral pH. *J. Soln. Chem* **18**, 705–725.

MOSES C. O., NORDSTROM D. K., HERMAN J. S., and MILLS A. L. (1987) Pyrite oxidation by dissolved oxygen and by ferric iron. *Geochim. Cosmochim. Acta* **51**, 1561–1571.

MOSES C. O., NORDSTROM D. K., and MILLS A. L. (1984) Sampling and analysing mixtures of sulphate, sulphite, thiosulphate and polythionate. *Talanta* **31**, 331–339.

NICHOLSON R. V., GILLHAM R. W., and REARDON E. J. (1988) Pyrite oxidation in carbonate-buffered solution: 1. Experimental kinetics. *Geochim. Cosmochim. Acta* **52**, 1077–1085.

NORDSTROM D. K. (1982) Aqueous pyrite oxidation and the consequent formation of secondary iron minerals. In *Acid Sulfate Weathering* (eds. L. R. HOSSAER et al.), Chap. 3. Soil Sci. Soc. Amer.

PLUMMER L. N., JONES B. F., and TRUESDELL A. H. (1976) WATEQF-A FORTRAN IV version of WATEQ, a computer program for calculating chemical equilibrium of natural waters. *US Geological Survey Water Resources Investigations Report No. 76-13.* (1984 revision is available.)

REYNOLDS R. L. and GOLDHABER M. B. (1978) Origin of a South Texas roll-type uranium deposit: I. Alteration of iron-titanium oxide minerals. *Econ. Geol.* **73**, 1677–1689.

SINGER P. C. and STUMM W. (1968) Kinetics of the oxidation of ferrous iron. *Proc. 2nd Symp. Coal Mine Drainage Res.*, pp. 12–34.

SINGER P. C. and STUMM W. (1970a) Acidic mine drainage: The rate-determining step. *Science* **167**, 1121–1123.

SINGER P. C. and STUMM W. (1970b) Oxygenation of ferrous iron. *Fed. Water Quality Admin. Rept. No. 14010-06/69.*

SMITH E. E., SVANKS K., and SHUMATE K. (1968) Sulfide to sulfate reaction studies. *Proc. 2nd Symp. Coal Mine Drainage Res.*, pp. 1–11.

SMITH E. E., SVANKS K., and SHUMATE K. (1970) Sulfide to sulfate reaction mechanism. *Fed. Water Quality Admin. Water Pollution Control Res. Study No. 14010-FPS-02-70.*

TAUBE H. (1984) Electron transfer between metal complexes: Retrospective. *Science* **226**, 1028–1036.

THORNBER M. R. (1975) Supergene alteration of sulphides. *Chem. Geol.* **15**, 1–14, 117–144.

TORAN L. (1987) Sulfate contamination in groundwater from a carbonate-hosted mine. *J. Contam. Hydrol.* **2**, 1–29.

WEHRLI B. and STUMM W. (1989) Vanadyl in natural waters: Adsorption and hydrolysis promote oxygenation. *Geochim. Cosmochim. Acta* **53**, 79–77.

WIERSMA C. L. and RIMSTIDT J. D. (1984) Rates of reaction of pyrite and marcasite with ferric iron at pH 2. *Geochim. Cosmochim. Acta* **48**, 85–92.